2019 IEEE Pacific Visualization Symposium (PacificVis)

Analysis of coupled thermo-hydro-mechanical simulations of a generic nuclear waste repository in clay rock using fiber surfaces

Christian Blecha
Institute of Computer Science
Leipzig University
Leipzig, Germany
blecha@informatik.uni-leipzig.de

Felix Raith
Institute of Computer Science
Leipzig University
Leipzig, Germany
raith@informatik.uni-leipzig.de

Gerik Scheuermann
Institute of Computer Science
Leipzig University
Leipzig, Germany
scheuer@informatik.uni-leipzig.de

Thomas Nagel
Chair of Soil Mechanics and Foundation Engineering,
Institute of Geotechnics
Technische Universität Bergakademie Freiberg
Freiberg, Germany
Thomas.Nagel@ifgt.tu-freiberg.de

Olaf Kolditz
Department of Environmental Informatics
Helmholtz Center for Environmental Research
Leipzig, Germany
olaf.kolditz@ufz.de

Jobst Maßmann
Federal Institute for Geosciences and Natural Resources (BGR)
Hannover, Germany
Jobst.Massmann@bgr.de

***Abstract*—The use of clean and renewable energy and the abandoning of fossil energy have become goals of many national and international energy policies. But even when once accomplished, mankind has to take charge of the relics of the current energy supply system. For example, due to its harmful effects, nuclear waste has to be isolated from the biosphere safely and for sufficiently long times. The geological subsurface is considered as a promising option for the deposition of such by- or end products. In order to investigate the long-term evolution of a repository system, a multiphysics simulation was performed. It combines the structural mechanics of the host rock, the fluid dynamics of formation fluids, and the thermodynamics of all materials resulting in a highly multivariate data set. A visualization of such multiphysics data challenges the current methodology. In this article, we demonstrate how an analysis of a carefully selected subset of the variables in attribute space allows to visualize and interpret the simulation data. We apply a fiber surface extraction algorithm to explore the relationships between these variables. Studying the temporal evolution in attribute space, we found a regionally bulge that could be identified as an effect of the nuclear waste repository because it can be clearly separated from the natural geophysical state prior to waste disposal. Furthermore, we used the extracted fiber surface as a starting point to examine the distribution of other variables inside this area of the physical domain. We conclude this case study with lessons learned from the visualization as well as the geotechnical side.**

***Keywords*-visualization, multiphysics, geology, fiber surface, interaction**

I. Introduction

An increasing number of scientific and engineering problems require an approach to their solution that crosses traditional disciplinary boundaries. Even when not taking into account economic, societal, and other nontechnical aspects, this is still the case considering the physical analysis per se of a natural or technical system. The reason for this development is that the functioning of natural systems in general and of an increasing number of designed technical systems rests on the interaction between multiple physical processes. Thermal, mechanical, fluid dynamic, electrical, magnetic, and even chemical or biological phenomena may need to be considered to understand or control the functioning of certain technologies such as biomedical devices, geothermal power plants, intelligent sensors and actuators, high-performance thermal systems for the thermodynamic regulation of jet or rocket engines, and novel smart materials, to name just a few.

Engineers use numerical simulations based on mathematical models to gain an understanding of how these multiphysical phenomena interact and to design such interactions for particular purposes. Extracting useful information from such complex simulation results from which a whole plethora of calculated quantities emerges, remains a challenge. In this paper, we test a visualization approach based on fiber surfaces by applying it to the analysis of a multiphysical simulation of a deep geological repository. We consider this application as a typical example of such multiphysical data sets and derive some lessons for similar data sets.

II. Motivation

The usage of the geological subsurface is increasing considerably in its intensity and diversity. Major associated requirements result from the exploitation of renewable as well as conventionally and unconventionally harvested traditional energy carriers, the short and long-term storage of energy carriers and energy, as well as the deposition of by- or end products of the energy supply system. This increasing

2165-8773/19/$31.00 ©2019 IEEE
DOI 10.1109/PacificVis.2019.00030

and sometimes competing use of the subsurface can cause usage conflicts and raises questions regarding the technical safety, the associated environmental impact as well as the societal acceptance [1], [13].

The detection, description, and assessment of anthropogenic intervention into the terrestrial environment, especially the geological subsurface, require competencies from the environmental, engineering and earth sciences, as well as from geotechnics. This extends in particular to one of the central challenges society as a whole faces this century — the search, construction, and operation of a repository to host nuclear waste with the best possible safety.

The emplacement of heat-emitting nuclear waste into deep geological repositories leads to perturbations of the natural in-situ state of the target formation. This perturbation develops over time as the decaying radioactivity produces heat and involves changing stress regimes, pressurization and hence flow of formation fluids, the temperature increase in the host rock, chemical alterations, among others.

Regulations require that analyses of the long-term safety be performed to demonstrate that no unwanted consequences arise as a result of the waste disposal. In particular, no harmful amounts of radionuclides are allowed to reach the biosphere.

A wide range of physical and chemical processes interact in the subsurface as a result of nuclear waste disposal [25]. For example, the transport of radionuclides depends on the flow regime, which in turn depends on temperature fields, deformation processes, the activation of fault zones, chemical alterations to the geotechnical barriers and host rocks, etc.

Therefore, numerical analyses are performed, which take into account the current knowledge of the involved relevant processes as well as their interactions and aim at assessing the long-term evolution of the repository system for various sets of boundary conditions, complementing assumptions, and so on. These models also allow the identification of crucial parameters which govern system evolution and provide hints for repository design or monitoring strategies.

As a result of the inherent complexity of the advanced process models, the analysis of the simulation results is a challenging task. This is exacerbated by the geometrical complexity and the size of the modeled geological system as well as its temporal evolution over centuries. Visual approaches geared towards exploring the geometrical and physical domains in their mutual context are therefore powerful tools in the hands of an analyst.

A. Questions

The engineers modeling the nuclear waste repository are interested in answering the following questions, e.g.:

- Is the repository safe, i.e. can we rule out the possibility of a harmful release of radionuclides into the biosphere?
- How large is the human impact on persistent natural gradients of relevant variables (e.g. temperature, hydrostatic pressure)?
- How high is the probability that new rock defects will occur? How does this affect the flow of the formation fluid, especially the radionuclide transport?

But, there are also issues that are more open and require exploratory data analysis:

- How do we decide which quantities to look at first in the analysis?
- How to advance from a simple overview to more complex questions, such as the likelihood of failure?
- How to find regions and time steps of interest, even if they are far away from the obvious center of attention?

We will come back to these questions in the discussion after we described the underlying simulation model and the visualization techniques used.

III. Model

For this study, an analysis of a generic, i.e. *non*-site-specific, nuclear waste repository in a claystone/ clayey marl formation (see Fig. 2.6 [12, p. 21] and Fig. 2.7 [12, p. 22]) typical of Northern Germany, previously analyzed as part of the ANSICHT project [10]–[12], was chosen as a representative example for the thermo-hydro-mechanical (THM) analysis of subsurface systems.

The numerical model consisted of eleven geological layers each with their own material properties. Initially, the system is characterized by a temperature distribution in line with the geothermal gradient, hydrostatically increasing fluid pressures, and a stress field determined by gravity and the tectonic state.

The simulation started with the excavation of the repository area in the target formation which alters the stress as well as the fluid pressure distribution (see Fig. 2.4 [12, p. 18]). This is followed by the waste emplacement and continued with the subsequent post-closure phase. During the latter, prescribed heat sources were applied to represent the waste packages in the repository.

To simulate the processes triggered by this heat input, the process model chosen was a so-called thermo-hydro-mechanical model, capturing the rock deformations and fluid motion as a result of the evolving temperature fields and altered boundary conditions. The scientific open-source finite element software OpenGeoSys [15] was used to simulate the system evolution by solving the following set of equations:

The *mass balance* considered effects of fluid and solid grain compressibility, $\beta_{p\mathrm{W}}$ and K_{SR}^{-1}, fluid and solid thermal expansivity, $\beta_{T\mathrm{W}}$ and $3\alpha_{\mathrm{S}}$, respectively, and fluid and solid volume change derived from the displacement field $\mathbf{u}$ on the

flow and pressure fields:

$$\left(\phi\beta_{p\mathrm{W}} + \frac{\alpha_\mathrm{B} - \phi}{K_\mathrm{SR}}\right)\frac{\mathrm{d_S}p}{\mathrm{d}t} - \left[\phi\beta_{T\mathrm{W}} + 3\alpha_\mathrm{S}\left(\phi - 1\right)\right]\frac{\mathrm{d_S}T}{\mathrm{d}t}$$
$$-\mathrm{div}\left[\frac{\mathbf{k}}{\mu_\mathrm{WR}}\left(\mathrm{grad}\, p - \rho_\mathrm{WR}\mathbf{g}\right)\right] + \alpha_\mathrm{B}\mathrm{div}\,\frac{\mathrm{d_S}\mathbf{u}}{\mathrm{d}t} = 0 \quad (1)$$

Darcy's law has been substituted with $\mathbf{k}$ being the intrinsic permeability tensor, μ_WR the fluid viscosity, p the fluid pressure, ρ_WR the fluid density, $\mathbf{g}$ the gravity acceleration vector, ϕ the porosity, and α_B Biot's coefficient. The material time derivative following the motion of the solid skeleton is expressed by $\mathrm{d_S}(\bullet)/\mathrm{d}t$.

The *energy balance* takes into account heat storage via the specific heat capacities c_p of the fluid (W) and the solid (S), conductive heat transport via the heat conductivity tensors $\boldsymbol{\lambda}$ of fluid and solid, and advective heat transport by the fluid given here by the term containing Darcy's law and the temperature gradient.

$$\left[\phi\,\rho_\mathrm{WR}\,c_{p\mathrm{W}} + (1-\phi)\rho_\mathrm{SR}\,c_{p\mathrm{S}}\right]\frac{\mathrm{d_S}T}{\mathrm{d}t}$$
$$-\mathrm{div}\,\left[\left(\phi\boldsymbol{\lambda}_\mathrm{WR} + (1-\phi)\boldsymbol{\lambda}_\mathrm{SR}\right)\mathrm{grad}\,T\right]$$
$$-\rho_\mathrm{WR}c_{p\mathrm{W}}\frac{\mathbf{k}}{\mu_\mathrm{WR}}\left(\mathrm{grad}\, p - \rho_\mathrm{WR}\mathbf{g}\right)\cdot\mathrm{grad}\,T = Q_T \quad (2)$$

Q_T denotes volumetric heat sources.

To solve for displacements, the *equilibrium conditions* were written as follows:

$$\mathrm{div}\,\left(\boldsymbol{\sigma}' - \alpha_\mathrm{B}p\mathbf{I}\right) + \left[\phi\rho_\mathrm{WR} + (1-\phi)\rho_\mathrm{SR}\right]\mathbf{g} = \mathbf{0}$$
$$\text{with}\quad \boldsymbol{\sigma}' = \mathcal{C} : (\boldsymbol{\epsilon} - \alpha_\mathrm{S}\Delta T\mathbf{I}), \quad (3)$$

Here, the effective principal stress has been used (extended for compressible solid grains). The effective stress $\boldsymbol{\sigma}'$ is calculated based on a linear-elastic material law, where the total strain tensor $\boldsymbol{\epsilon}$ is diminished by thermal strains, and where the fourth-order stiffness tensor $\mathcal{C}$ characterizes a transversally isotropic material.

Note that besides the apparent direct coupling terms in the above equations, further process coupling and nonlinearity are introduced by the dependence of material parameters and field quantities on the evolving primary solution fields. Examples are temperature-dependent heat conductivities, strain-dependent permeabilities, temperature- and pressure-dependent densities, etc.

For more details regarding the model, its context and the used parameters, see [10]–[12], for details regarding the nomenclature of the physical variables refer to, e.g., [16], [18].

Initial target measures in the analysis were temperature T, fluid pressure p, and the equivalent effective stress σ'_eq defined by

$$\sigma'_\mathrm{eq} = \sqrt{\frac{3}{2}\mathrm{dev}\,\boldsymbol{\sigma}' : \mathrm{dev}\,\boldsymbol{\sigma}'} \quad (4)$$

This choice was made as each of these variables is a scalar measure of the three main processes involved.

IV. Related Work

Visual exploration of multivariate data has been studied for about two decades. Blass et al. [2] used linked physical and feature space views to assist physicians in their exploration of the vast amount of medical data defined on the same physical domain. This data was produced by diffusion tensor imaging, computer tomography, and positron emission tomography. It also includes data derived as features based on the imaging data. Their main target was to use multiple data sets to improve the separation of points in the physical space which is used for example in virtual colonoscopy. One of the important steps during this examination is the extraction of the colon surface to identify polyps. It is difficult to clearly identify this surface using only CT data because of the misclassification of the air-contrast-boundary due to the partial volume effect. After the introduction of some new derived features based on the physical neighborhood of the data points, the extraction of the colon wall was improved. Also, they used linked two-dimensional views (e.g. scatter plots, sectional planes, histograms) to show directly the data defined on some selected measuring points.

Fuchs and Hauser [7] wrote a survey about the visualization of multivariate scientific data where they described some visualization techniques, which were mostly invented for scalar, vector or tensor fields. Furthermore, they showed the advantages of these techniques if they are applied to multivariate data. They gave an overview categorizing the presented techniques to identify main approaches for the handling of multivariate scientific data. The main examples were glyph rendering, interaction with the visualizations, like alteration of transfer functions or the selection of regions of interests inside the range, the use of multiple as well as n-dimensional views, and hybrid rendering. The last point describes the proper selection of a rendering algorithm for each displayed feature, which fits best.

A Dagstuhl seminar on visualization in 2011 [6] discusses current research challenges and summarizes the state of the art. One of the challenges is the visualization of multivariate data. In the collection, the work of David et al. [5] presents glyphs as an important technique for the visualization of multivariate data. It gives an overview of the different ways of using glyphs and discusses critical design aspects. Besides, other works also clarify the importance of feature-based techniques as a method to analyze multivariate data [3], [21].

One of the few cases covering multiphysics is the analysis of cerebral aneurysms by Perdikaris et al. [22]. They extended ParaView to interactively work with the vast amount of data of flow-structure interactions in a high-fidelity, numerical simulation. This simulation observed the blood flow inside a brain aneurysm, and the structural integrity of

the arterial wall whereas the aneurysm itself was extracted with the help of magnetic resonance imaging. After the data loading and refinement process, they visualized the course of the blood using streamlines and the local stress on the arterial wall which highlighted areas of multiphysic interactions of the blood flow and the surrounding tissue boundary. Additionally, they integrated the simulated displacement of the tissue into the visualization. Their extension of ParaView could produce unknown insights about the temporal evolution of an aneurysm and help physicians to decide about treatment.

In general, it can be said that despite field data visualization being at the heart of scientific visualization for decades, most techniques refer to univariate data. The exploration of multi- or at least bivariate data sets is still a challenging research topic. A substantial contribution was made by Carr et al. [4]. They developed an algorithm for the interactive extraction of separating surfaces using a two-dimensional range. These surfaces are referred to as fiber surfaces, which are a compound of multiple fibers/ isolines for multiple two-dimensional isovalues. Basically, they are a highly relevant generalization of isosurfaces to bivariate data. Generally, the surfaces are the inverse image of a polygon in the range. Because of the continuous mapping of every point of the domain to a point in the range and vice versa, the polygons in the range define connected surfaces. To render these surfaces Carr et al. [4] introduced a fiber surface extraction algorithm based on the classical Marching Cubes technique, which uses a distance field as input. This field is defined by the distance of the image of every point to the nearest polygon in range.

Based on this work, Klacansky et al. [14] improved the performance by two magnitudes, making it feasible to use the technique for interactive exploration. The improvement is achieved by the use of octree-based domain subdivisions and precalculated look-up tables of all possible triangular characterizations in the sense of marching cubes. Nevertheless, in their case, the isovalue is an element of a two-dimensional codomain, which leads to the use of polylines for the definition of fiber surfaces in the domain.

Jankowai and Hotz [9] introduced feature level-sets and traits as a more general approach for the visualization of multivariate data. Some special cases of them are default isosurfaces and the fiber surfaces of Carr et al. [4]. The idea is that the user selects the values he wants to show, which need not be a value for each of the available variables. Jankowai and Hotz expanded this selection process and gave the user the opportunity not only to select single values but also to use traits. Traits can be a body of the dimensionality smaller or equal to the dimensionality of the used attribute space. Afterwards, they compute a distance field within this attribute space as the distance to the closest trait. This distance field will be projected back into the spatial domain, where a simple direct volume rendering approach or marching cubes can be used to visualize the corresponding feature level-sets. In the end, they applied their approach to three different multivariate data sets from a material, a flow fluid, and a hurricane simulation to demonstrate the flexibility of their method.

Sauber et al. [24] introduced multifield-graphs to visualize correlations between multiple three-dimensional scalar fields, which are defined on the same domain. They introduced their graph to give an overview over the vast amount of correlation fields because the number of them increases exponentially with the number of considered scalar fields. Therefore, each node of this graph corresponds to one correlation field which combines at least two different fields and shows two characteristic values which describe the specific correlation field. These values indicate whether a correlation field is worth it to calculate and to take a closer look at because it shows a great correlation.

Nagaraj et al. [20] improved the visualization of relationships between multiple scalar fields of Sauber et al. [24]. They introduced another comparison measure because the one of Sauber et al. emphasizes the minimum correlation between two scalar fields and could therefore hide some high correlations between some other scalar fields for a given position x inside the domain D.

Liu and Shen [17] take a slightly different approach. They use an association analysis for multivariate data sets by using association rules to generate a parallel coordinate plot. The plots are used to select isovalues, and the association scalar values.

In contrast to our work, they are only visualizing the relationships between multiple scalar fields. Our approach is not only to investigate these relations but also to show where they occur inside the physical domain. Furthermore, we can use the fiber surfaces of the physical domain to investigate the relations of other scalar fields inside regions of interest.

Another method to analyze multivariate data is from Jänicke et al. [8]. They identify important regions automatically using local statistical complexity that can be described by partial differential equations which differs from our interactive selection approach.

Nagaraj et al. [19] also introduced another way of dealing with multiple scalar fields. Their idea was that the interactions between the fields have to be considered to find interesting isovalues of one field. In general they are looking on the variation of the fields over the isosurfaces of a selected field. Opposed to our approach, they are showing isosurfaces based on one scalar field.

In this paper, the algorithm of Raith et al. [23] is used. It presents a general approach for the generation of interfaces in symmetrical, three-dimensional, second-order tensor fields. These surfaces are defined as fiber surfaces of the invariant space, i.e., as models of surfaces in the range of a complete set of invariants. This work is a generalization of the approach from Klacansky et al. [14] to three dimensions

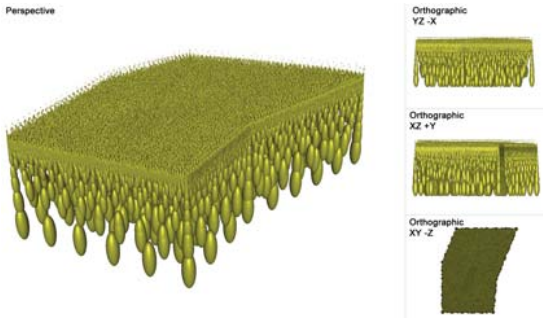

Figure 1. Direct Visualization of the principal stresses inside the data set ANSICHT [10]–[12] with ellipsoids.

in the range. Therefore, the assignment of the tensor field domain to the invariant space is an assignment of three-space to three-space, which allows a direct visualization of the invariant space. The work of Raith et al. [23] also enables a forward mapping from the domain to the invariant space. A careful look at the method reveals that it just requires three scalar fields, so it is not necessary for them to use a set of three invariants of one tensor field. Here, we use this approach with three scalar fields representing key measures of three important, physical quantities used in the simulation.

V. Direct Visualization attempt

Based on the survey of Fuchs and Hauser [7], a first attempt was made to analyze the data set. One of the simple possibilities is an analysis of the raw data, for example, by the extraction of statistical values like the maximum, minimum, median or the standard deviation. This allows for a rough overview of the data by statistical graphics like histograms, scatter plots, box plots, and so on. However, it does not allow to get answers to the engineering questions posed in section II-A.

To look into the spatial and temporal distribution of the values, scientific visualization is necessary. Therefore, according to the work of Fuchs and Hauser [7], we chose glyphs to display the multivariate data in our next attempt. They offer a good possibility to display several variables at the same time and to clarify their context. Fig. 1 shows the principal stresses from ANSICHT project, which is visualized using ellipsoids. Of course, ellipsoids are not an optimal choice to display multivariate values but any other glyph would also result in a similar overlapping problem. This does not allow to find important areas or to get an overview of the whole simulation. One might look for a clever glyph placement strategy, but basically, this means to detect the important positions in space and time first and to provide the required overview with even other means. Altogether, we came to the conclusion that we need a completely different strategy to start the visual analysis of the data.

VI. Visual Analysis

As mentioned, the visualization of large multivariate data is not simple, and there is no satisfying general solution so far. Here, we put the study of the relations between variables in attribute space at the heart of the method.

For this purpose, we built on the notion of *fiber surfaces* in the sense of Carr et al. [4] who study bivariate fields but we use the extension of Raith et al. [23] allowing for three scalar variables to be studied. (The actual paper by Raith et al. talks about three scalar invariants of a symmetric three-dimensional tensor of second order, but it turns out that the relation between the three scalars does not play any role for their algorithm.) Fiber surfaces combine the potential to be displayed continuously with the simplicity of isosurfaces, so that no feature will be missed due to overlap in attribute space, no wrong impression should arise due to the placement (like a regular placement of glyphs in a grid), or the variety of the encoded information would overcome the user.

The algorithm assumes a tetrahedral mesh representing physical space. At every grid point, the three variables define a point in the three-dimensional attribute space (the range):

$$\begin{aligned} f : \mathbb{R}^3 &\to \mathbb{R}^3 \\ x &\mapsto f(x) \end{aligned} \tag{5}$$

Assuming piecewise linear interpolation in physical space results in a mapping of the whole tetrahedral grid into attribute space. In other words, the structure and the neighborhoods are kept when the tetrahedral mesh is mapped from the three-dimensional physical into three-dimensional attribute space.

In the range, the user can select an *interactor*, i.e. a volumetric object defining a triangulated surface. Each point of this surface defines a value combination of the three scalar fields, which in general has a discrete set of points as pre-image. The piecewise linear nature of the fields means that the triangulated surface, i.e. the interactor, has a triangulated surface as pre-image – the fiber surface. It has similar properties to isosurfaces and can be used to study the common behavior of all three variables in the physical domain. As pointed out by Raith et al. [23], this algorithm can also be used to map a triangulated surface in physical space, enclosing some region of interest, into attribute space. We will also use this feature in our analysis.

Fuchs and Hauser [7] pointed out two main questions of multivariate field visualization:

1) What to visualize?
2) How to visualize?

Concerning the “what”, in this paper we consider the THM model. If we can find three representative scalar variables for this model, the fiber surfaces from Raith et al. [23] would be very useful. One can use the volumetric interactor to select areas in the data set with highly relevant combinations of

values of these variables. Otherwise, we would need either to generalize the method to even more fields or to restrict ourselves to three variables at a time and try to work with different sets of three variables.

The obvious question is: Which three variables should be used? One idea could be to use similar variables, which either means to group variables with a similar meaning or variables which refer to the same kind of physical process. This idea could lead to a better understanding of one physical process, which would be a proper way if each model is studied separately. However, the main questions of the engineers concern the interaction of the three kinds of processes. Therefore, the dependencies between thermodynamics, solid mechanics, and fluid dynamics are the focus of this application. The interactions between the three models have to be considered at the same time, to gain a real comprehension of the processes during the final disposal of radioactive material. In this paper, the following variables are used for the analysis:

- the equivalent effective stress σ'_{eq} in Pa (solid mechanics),
- the fluid pressure p in Pa (fluid dynamics), and
- the temperature T in °C (thermodynamics).

This selection reflects the multiphysics character of the underlying data set and was an almost immediate suggestion by the engineers.

Besides the selection of the three variables, the selection of the coordinate system is also important. As mentioned by Raith et al., this decision depends on the properties of the selected variables. Here, we selected a Cartesian coordinate system as no variable is measured as angle.

Furthermore, the visual impression depends on scaling the ranges of all variables. This is important because the whole tetrahedral mesh is visualized in attribute space. If ranges of variables are quite different, the mesh looks like a plane or line in attribute space. However, it would also be possible to define it automatically with the help of statistics. It should be noted that in some case, there is a non-linear scaling of values along the axes in the Figures.

As a first result, Fig. 2a shows a very early stage of the domain observed corresponding to the in-situ state. The visualization shows the expected behavior of a rise of the temperature due to the geothermal gradient as well as the fluid pressure according to an increase of the depth in the physical domain. After this point in time, the disturbance by the insertion of the repository for nuclear waste will be started and the repository will be filled and sealed afterwards. In Fig. 2b, we can see the state after 600 years. The inserted disturbance is clearly identifiable as a bulge that has formed adjacent to the natural state. According to Fig. 6c, where a cuboid interactor is used to cut the bulge from the natural state, the two inserted chambers for the repository are clearly recognizable as fiber surfaces inside the physical domain on the right side. Due to the fiber

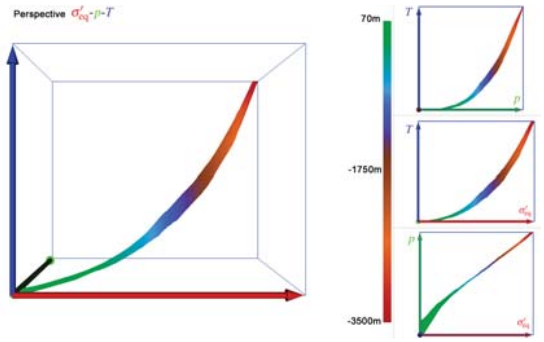

(a) $t = 0$ years

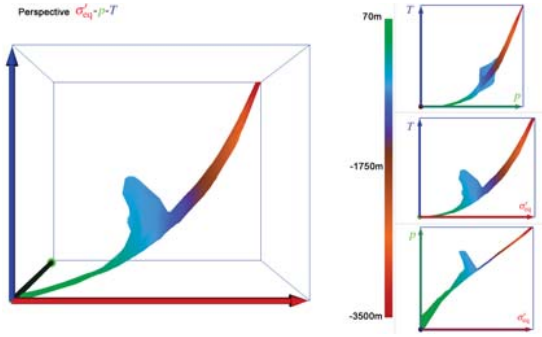

(b) $t = 600$ years

Figure 2. Coloring of the tetrahedral mesh in the attribute space according to the depth in physical space after t years.

surface extraction algorithm, the placing of the interactor, and the corresponding fiber surfaces, all tetrahedra of the bulge can be seen as part of the inserted repository. This means that this disturbance can clearly be seen inside the attribute space compared to the natural state of the system. The light blue coloring of the bulge in Fig. 2b confirms this statement as it shows that the increase in temperature, as well as fluid pressure, is not associated with a deeper position inside the physical domain but with the radioactive decay of the nuclear waste.

To include geology into the study, we use a coloring of the geological layers as given by Fig. 3. The original geological structure can be seen on the right side of Fig. 6c with this coloring. Here, the contour of the physical domain is shown with the material in every depth projected on slices through the domain as geographical background information. In Fig. 4, we look again at the in-situ state of the future repository area. Here, we can clearly see that temperature, pressure, and effective stress all raise according to the layering as given in Fig. 6c. Looking at the state 600 years later (in Fig. 4b), we can confirm that the material of the repository (orange-red color) is inside the bulge. It also becomes clear which part of the surrounding of the repository undergoes substantial change.

Figure 3. Legend of the materials from the ANSICHT project used in Fig. 4 and following. For information on the materials, see [10]–[12].

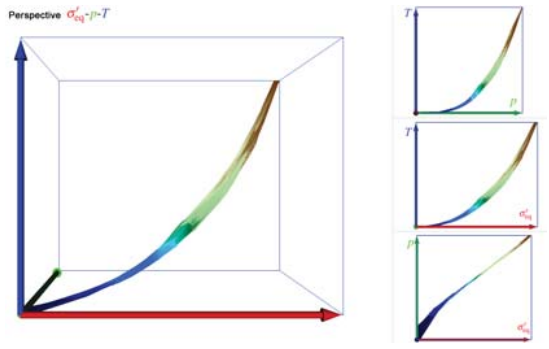

(a) $t = 0$ years

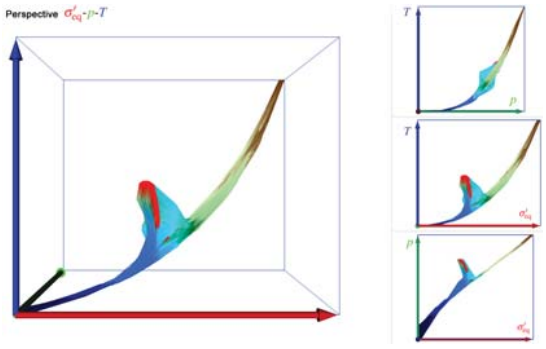

(b) $t = 600$ years

Figure 4. Coloring of the tetrahedral mesh in the attribute space according to the geological layer the element belonged to in physical space at two time points during the simulation. For information on the geological layers, see [10]–[12] and Fig. 3. Orange-red marks the tetrahedra whose material belong to the inserted repository.

VII. Visual Analysis over Time

As the main purpose of the model is to study the development of the geological structure and the impact of the nuclear waste repository over time, a temporal analysis is the key. Due to the already described problems with glyphs, they are not suitable for temporal analysis. But a temporal overview about the change of individual variables and also their interaction is important to understand the processes inside such a multiphysics data set. Therefore, we created a cartoon with manually chosen time steps in Fig. 6a to Fig. 7c. The time steps do not increase linearly depending on the simulation. There are two reasons for this. Firstly, the simulation does not write out each time step after fixed duration. Secondly, there is basically no change in the data in the first 20 years, and in the years from 65,000 till the end (1,000,000 years). This time limitation highly depends on the distance metric, which is used to compare the tetrahedral grid in attribute space of time n with that of time 0. In this case a tetrahedron is classified as *'has changed'* if the difference vector of the position vectors of at least one corner point, is in not less than one component smaller or equal than a user-defined vector of distances (here: $\boldsymbol{v} = (\ 100\ \text{Pa},\ 100\ \text{Pa},\ 5\ \text{K}\ )^T$).

All images show the tetrahedral mesh in attribute space on the left-hand side with a cuboid interactor as the green wire-frame. Position, size, and orientation of this interactor do not change during the analysis. Furthermore, the parts of the mesh which differ at a specific time from the first image are highlighted in yellow. This means that the yellow parts of the mesh show tetrahedra whose positions in attribute space at time t (with $t > 0$) differs from the initial state at $t = 0$. (The occurrence of blue parts inside the yellow bulge is only due to some clipping errors because of the simultaneous rendering of two grids at the same position.) The lack of yellow mesh parts outside the bulge confirms the fact, that this local bulge contains the whole disturbance, which is a major insight for the engineers.

On the right-hand side of the images, the physical domain is shown as a contour of the whole mesh to reduce clutter. To facilitate the geographical classification of the fiber surfaces, two sectional planes are inserted. They show the correlation of the depth and the geological layer (i.e. the material) according to Fig. 3.

During the temporal evolution of the system, the bulge forms starting from scratch in the natural state, over a large expansion phase until 600 years, and goes back to natural state after 65,000 years. As soon as the bulge is large enough to penetrate the boundary of the interactor, the corresponding fiber surfaces are extracted. For example in Fig. 6b, the two chambers of the repository are clearly visible in physical space even if the bulge is still small. To encode more information inside the physical space, the fiber surfaces are colored by the temperature.

Due to the consistent position of the interactor over time, the fiber surfaces for the same isovalues are shown at each time step. Therefore, the growth of the fiber surfaces indicates the effect of the radioactive decay of the nuclear waste, which raises the temperature, then the fluid pressure, and finally alters the effective stress. So the rock mass surrounding the chambers warms up, which leads to a translation of the surface, which corresponds to the chosen temperatures (isosurface). After all the heat emission from the decaying radioactive waste has gone, the temperature, as well as the other values, decrease, which can be seen in Fig. 7b. The missing fiber surfaces at this time step indicate that the remaining impact is also very small. This can be confirmed by the back transformation of the yellow

colored grid parts to the natural state in attribute space (again indicating the change compared to the initial state). Regarding the other time steps it can be concluded that the bulge will retract and that the initial state will be reached again.

VIII. Insights by Engineers

The clear link between the primary results of the thermo-hydro-mechanical analysis, i.e. between temperature, fluid pressure, and effective stress, proved very useful for the analysis of the *coupled* process, rather than of each individual process at a time.

At the onset of modeling, i.e. in the natural state, one observes a clear correlation between the depth-dependent temperature field associated with the geothermal gradient, the depth-dependent hydrostatic pore pressure field, and the depth-dependent stress field due to the specific gravity of the rock mass with a slight influence of nonlinearity due to state-dependent properties.

The interactor is empty, hence no region of interest is highlighted in the Euclidean view.

Once the heating phase commences, a bulge forms in the σ'_{eq} - p - T state space indicating very clearly the perturbation of the natural geological system. All three quantities are altered. This perturbation lies within the interactor causing a bounding surface to appear in the Euclidean panel, which encloses all points lying in the perturbed region. It is clearly evident that the highlighted zone corresponds to a zone of influence surrounding the repository properly.

Over time, the perturbation — and with it the influenced spatial domain — shrinks, such that the system eventually returns to its natural state (gradients).

This visualization has several advantages: The perturbation in a chosen state space, here composed of equivalent effective stress, fluid pressure, and temperature, is clearly visible in terms of its relative magnitude with respect to the pre-existing natural/ in-situ state. This allows an immediate intuitive judgment of the severity of the anthropogenic intervention. Additionally, due to the intrinsic correlation of the natural state with the depth, the state space plot roughly indicates the depth of the perturbation. The three planar projections of the three-dimensional illustration allow viewing selected two-variable relations, and an easier quantitative assessment. The interactor allows a user-interactive exploration of where the perturbed zone (or any other state space region, for that matter) lies in the physical Euclidean object space. Provided some context, here given by the view of the stratigraphic geological layers, this again allows an immediate intuitive assessment, this time of the geometrical extent of the selected region, in this case, the anthropogenic perturbation.

Based on this initial assessment derived from studying one characteristic quantity per coupled process simultaneously, the main region of interest could be identified. It is not obvious, however, if other important regions could be missed that are associated with other key measures. To study this further, a second forward mapping was performed by placing an interactor within the found ROI and plotting a number of attribute spaces, cf. Fig. 5. Here, the chosen spaces serve as an illustration and have been selected to provide more information on the structural integrity of the rock material. Briefly, the upper left figure comprised the principal effective stress space allowing the identification of maximum compressive or tensile loading. The upper right figure shows a space composed of temperature, vertical displacement and $b = \sigma'_{\mathrm{eq}}/\bar{\sigma}'$ showing how temperature, uplift and the strength-related ratio of equivalent over mean effective stress interact. The stress space composed of hydrostatic effective stress, equivalent effective stress and Lode angle – measure of the mode of loading describing the orientation of the stress state in the deviatoric plane – in the lower left figure provides information on deviatoric vs. isotropic stress magnitudes and the mode of loading. The last space connects the temperature, the Lode angle and the equivalent to mean effective stress ratio. Note, that any scalar failure measure derived from hyper-surfaces in stress- or strain-space can be included here.

The green region highlights the values occupied by the previously identified region of interest based on the initially chosen quantities characterizing the coupled process. The blue region shows all numerical values that occur in the model. By comparing the blue and green domains, it can be observed whether the most critical or interesting values in the respective attribute space coincide with the preselected ROI, or whether certain extreme values lie outside of the domain. For example, temperature gradients or far-field pressure signals, as well as material interfaces, can induce critical stress conditions at some distance from the repository domain itself.

By identifying interesting spots in the blue shaded areas, one can again go back to the Euclidean space to see where such effects may occur. Thus, one development goal for the future should be a seamless switching between attribute (phase) space and physical (Euclidean) space in order to achieve a quick build-up of an understanding of the model results. For this purpose, a wide range of analysis quantities of interest to the engineer should be available, as demonstrated in Fig. 5.

IX. Lessons for Visualization Research

Overall, the visual analysis of this multiphysics data set using linked views of physical and attribute space was a success. This can be seen from the comment: “This allows an immediate intuitive judgment of the severity of the anthropogenic intervention.” by the engineer who wrote the previous section. Besides the simple description of natural state and anthropogenic impact, the fiber surfaces also allow

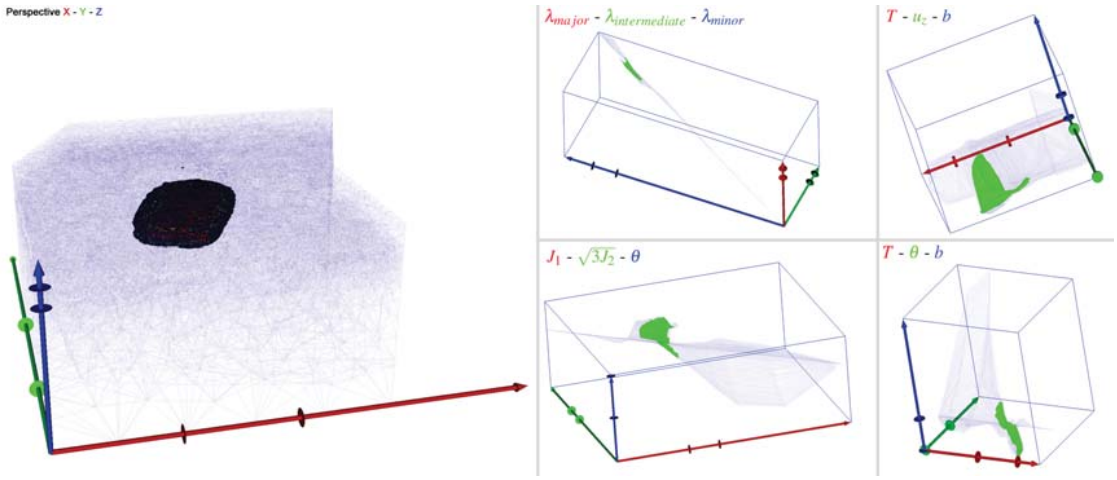

Figure 5. Extended sets of attribute spaces derived from the fiber surface associated with the original attribute space. An interactor is placed inside the fiber surface on the left-hand side (black surface). It is used for the extraction of the fiber surfaces in each of the four spaces on the right-hand side respectively.

for an effective analysis of further variables in the regions showing man-made changes.

If we look back at the original questions of the engineers, it can be seen that they were able to judge the safety of the repository, assess the magnitude of anthropogenic impact in relation to the natural state, and get at least some idea on the probability of rock faults and radionuclide transport into the biosphere by studying additional variables in the ROI defined by the bulge. They got a clear indication of where to start their analysis, because we presented a simple overview as a starting point for additional analysis, and found regions and time steps of interest.

However, any other multiphysics simulation data set may differ substantially in used physical models, variables of interest, and basic questions. This raises the question what can be learned from this example. We see three main lessons to draw.

One insight from this study is based on the fact that the simulation uses three coupled physical models, i.e. thermodynamics, fluid dynamics, and structural mechanics. Here, it proved useful to look for one (scalar) variable for each model to judge the results of this model in the best way. This allowed to study the relations between the different physical models by looking at only three variables. Of course, one may complement this with visualizations that look only at the individual models, e.g. using results of flow visualization or structural mechanics visualization in the literature.

The second insight is based on the well-known fact that large and complex data requires a good overview. A good overview is often difficult to accomplish, so it is worth to note the two key factors of success in this example. First factor: the attribute space provides a very good overview of the relation between the three selected variables in the natural state. The engineers know about the natural relation between temperature, fluid pressure, and solid stress, which basically all increase with depth due to gravity. This is a key feature to interpret a rather abstract view like the attribute space and to really rely on it. Second factor: the anthropogenic influence, i.e. the key question, can be studied quite easily in attribute space, and it can be judged directly in relation to the natural state. Again, this fact allows for fast and faithful interpretation of the results in this case. Together with the possibility to link the change in attribute space to the region in physical space, this allowed the engineers to study their results in a nice fashion. By the way, the faith of the engineers in the implementation was partly built by validating that the change is associated with the deposit chambers in the early time steps (the information about the chambers was not given to the visualization team in the beginning).

The final insight is again well-known in theory, but sometimes a challenge: Allow for inspection of details. In the study, many variables and effects were neglected for the overview by only looking at three variables. These variables allow to see where and when changes occur and to judge the danger of the nuclear waste deposit coarsely, but in-depth analysis requires to study other variables as well. Here, the fiber surfaces helped by defining the spatial (and temporal) domain of interest in a user-friendly manner. Using the fiber surfaces in the physical domain as interactor, it is very simple to select other variables and study their values in attribute space, including a look for extreme values outside the regions defined by the selected three variables. Obviously, this feature is very important as mentioned by the engineer — otherwise, the analysis could miss dangerous developments outside the surrounding of the repository.

We believe that these three lessons, i.e. a careful selection of representative variables for each physical model, an

overview of natural state and human impact in attribute space, and looking at the remaining variables based on the found spatial regions and timesteps, give some guidance on similar multiphysics applications, at least in the environmental research domain.

X. Conclusion

In this application paper, we present a successful visual analysis of a multiphysics simulation of a nuclear waste repository. The simulation results in a large, highly multivariate data set that is difficult to study due to many nonlinear effects in the model. We demonstrate that the fiber surface algorithm by Raith et al. [23] allows creation of a very effective overview visualization in this case. This is due to the fact that the engineers could select three scalar variables describing the effects of thermodynamics, fluid dynamics, and structural mechanics on the geological structure. As can be seen from the original questions from and the insights gained by the engineers, a state-space analysis of these three variables let to a clear mental overview of the whole simulation process, and a coarse judgment of the anthropogenic impact of the repository. Guided by the fiber surfaces, the engineers were able to look deeper into the change in the rock using additional variables. For the visualization of similar multiphysics data sets, especially from environmental sciences, we concluded that a careful selection of representative variables for each physical model, creating an overview of natural state and human impact in attribute space, and looking at the remaining variables based on the found spatial regions and time steps, provides some guidance.

Acknowledgment

The Federal Institute for Geosciences and Natural Resources (BGR) is a technical and scientific agency of the Federal Ministry for Economic Affairs and Energy (BMWi). The authors would like to thank the BMWi for funding the ANSICHT project, which provided the data base for this study. This work was funded by the German Federal Ministry of Education and Research within the project *Competence Center for Scalable Data Services and Solutions* (ScaDS) Dresden/Leipzig (BMBF 01IS14014B).

References

[1] S. Bauer, A. Dahmke, and O. Kolditz. Subsurface energy storage: geological storage of renewable energy—capacities, induced effects and implications. *Environmental Earth Sciences*, 76(20):1–4, 2017. doi: 10.1007/s12665-017-7007-9

[2] J. Blaas, C. P. Botha, and F. H. Post. Interactive visualization of multi-field medical data using linked physical and feature-space views. In *Proceedings of Eurographics - IEEE VGTC Symposium on Visualization '07*, pp. 123–130, 2007.

[3] H. Carr. Feature Analysis in Multifields. In *Scientific Visualization: Uncertainty, Multifield, Biomedical, and Scalable Visualization*, Mathematics and Visualization, pp. 197–204. Springer, 2014.

[4] H. Carr, Z. Geng, J. Tierny, A. Chattopadhyay, and A. Knoll. Fiber surfaces: Generalizing isosurfaces to bivariate data. *Computer Graphics Forum*, 34(3):241–250, 2015. doi: 10.1111/cgf.12636

[5] D. H. Chung, R. S. Laramee, J. Kehrer, and H. Hauser. Glyph-based multi-field visualization. In *Scientific Visualization*, pp. 129–137. Springer, 2014.

[6] C. D. Hansen, M. Chen, C. R. Johnson, A. E. Kaufman, and H. Hagen. *Scientific Visualization: Uncertainty, Multifield, Biomedical, and Scalable Visualization*. Mathematics and Visualization. Springer, 01 2014.

[7] R. Fuchs and H. Hauser. Visualization of multi-variate scientific data. *Computer Graphics Forum*, 28(6):1670–1690, 2009.

[8] H. Janicke, A. Wiebel, G. Scheuermann, and W. Kollmann. Multifield visualization using local statistical complexity. *IEEE Transactions on Visualization and Computer Graphics*, 13(6):1384–1391, 2007.

[9] J. Jankowai and I. Hotz. Feature level-sets: Generalizing iso-surfaces to multi-variate data. PP:1–1, 09 2018.

[10] M. Jobmann, A. Bebiolka, V. Burlaka, P. Herold, S. Jahn, A. Lommerzheim, J. Maßmann, A. Meleshyn, S. Mrugalla, K. Reinhold, A. Rübel, L. Stark, and G. Ziefle. Safety assessment methodology for a German high-level waste repository in clay formations. *Journal of Rock Mechanics and Geotechnical Engineering*, 9(5):856–876, oct 2017. doi: 10.1016/J.JRMGE.2017.05.007

[11] M. Jobmann, A. Bebiolka, S. Jahn, A. Lommerzheim, J. Maßmann, A. Meleshyn, S. Mrugalla, K. Reinhold, A. Rübel, L. Stark, and G. Ziefle. Sicherheits- und Nachweismethodik für ein Endlager im Tongestein in Deutschland. Synthesebericht. Technical report, 2017.

[12] M. Jobmann, V. Burlaka, P. Herold, E. Kuate Simo, J. Maßmann, A. Meleshyn, A. Rübel, and G. Ziefle. Projekt ANSICHT Systemanalyse für die Endlagerstandortmodelle Methode und exemplarische Berechnungen zum Sicherheitsnachweis. Technical report, 2017. doi: 10.15713/ins.mmj.3

[13] A. Kabuth, A. Dahmke, C. Beyer, L. Bilke, F. Dethlefsen, P. Dietrich, R. Duttmann, M. Ebert, V. Feeser, U.-J. Görke, R. Köber, W. Rabbel, T. Schanz, D. Schäfer, H. Würdemann, and S. Bauer. Energy storage in the geological subsurface: dimensioning, risk analysis and spatial planning: the ANGUS+ project. *Environmental Earth Sciences*, 76(1):23, jan 2017. doi: 10.1007/s12665-016-6319-5

[14] P. Klacansky, J. Tierny, H. Carr, and Z. Geng. Fast and exact fiber surfaces for tetrahedral meshes. *IEEE Transactions on Visualization and Computer Graphics*, 23(7):1782–1795, July 2017. doi: 10.1109/TVCG.2016.2570215

[15] O. Kolditz, S. Bauer, L. Bilke, N. Böttcher, J. O. Delfs, T. Fischer, U. J. Görke, T. Kalbacher, G. Kosakowski, C. I. McDermott, C. H. Park, F. Radu, K. Rink, H. Shao, H. B. Shao, F. Sun, Y. Y. Sun, A. K. Singh, J. Taron, M. Walther, W. Wang, N. Watanabe, Y. Wu, M. Xie, W. Xu, and B. Zehner. OpenGeoSys: an open-source initiative for numerical simulation of thermo-hydro-mechanical/chemical (THM/C) processes in porous media. *Environmental Earth Sciences*, 67(2):589–599, sep 2012. doi: 10.1007/s12665-012-1546-x

[16] O. Kolditz, T. Nagel, H. Shao, W. Wang, and S. Bauer, eds. *Thermo-Hydro-Mechanical-Chemical Processes in Fractured Porous Media: Modelling and Benchmarking*. Terrestrial Environmental Sciences. Springer International Publishing, Cham, 2018. doi: 10.1007/978-3-319-68225-9

[17] X. Liu and H.-W. Shen. Association analysis for visual exploration of multivariate scientific data sets. *IEEE transactions on visualization and computer graphics*, 22(1):955–964, 2016.

[18] X.-Y. Miao, C. Beyer, U.-J. Görke, O. Kolditz, H. Hailemariam, and T. Nagel. Thermo-hydro-mechanical analysis of cement-based sensible heat stores for domestic applications. *Environmental Earth Sciences*, 75(18):1293, sep 2016. doi: 10.1007/s12665-016-6094-3

[19] S. Nagaraj and V. Natarajan. Relation-aware isosurface extraction in multifield data. *IEEE Transactions on Visualization and Computer Graphics*, 17(2):182–191, Feb 2011. doi: 10.1109/TVCG.2010.64

[20] S. Nagaraj, V. Natarajan, and R. S. Nanjundiah. A gradient-based comparison measure for visual analysis of multifield data. *Computer Graphics Forum*, 30(3):1101–1110, 2011. doi: 10.1111/j.1467-8659.2011.01959.x

[21] H. Obermaier and R. Peikert. Feature-Based Visualization of Multifields. In *Scientific Visualization: Uncertainty, Multifield, Biomedical, and Scalable Visualization*, Mathematics and Visualization, pp. 189–196. Springer, 2014.

[22] P. Perdikaris, J. A. Insley, L. Grinberg, Y. Yu, M. E. Papka, and G. E. Karniadakis. Visualizing multiphysics, fluid-structure interaction phenomena in intracranial aneurysms. *Parallel Computing*, 55:9 – 16, 2016. Visualization and Data Analytics for Scientific Discovery. doi: 10.1016/j.parco.2015.10.016

[23] F. Raith, C. Blecha, T. Nagel, F. Parisio, O. Kolditz, F. Günther, M. Stommel, and G. Scheuermann. Tensor field visualization using fiber surfaces of invariant space. *IEEE Transactions on Visualization and Computer Graphics*, pp. 1–1, 2018. doi: 10.1109/TVCG.2018.2864846

[24] N. Sauber, H. Theisel, and H. Seidel. Multifield-graphs: An approach to visualizing correlations in multifield scalar data. *IEEE Transactions on Visualization and Computer Graphics*, 12(5):917–924, Sep. 2006. doi: 10.1109/TVCG.2006.165

[25] C. Tsang, J. Barnichon, J. Birkholzer, X. Li, H. Liu, and X. Sillen. Coupled thermo-hydro-mechanical processes in the near field of a high-level radioactive waste repository in clay formations. *International Journal of Rock Mechanics and Mining Sciences*, 49:31–44, jan 2012. doi: 10.1016/j.ijrmms.2011.09.015

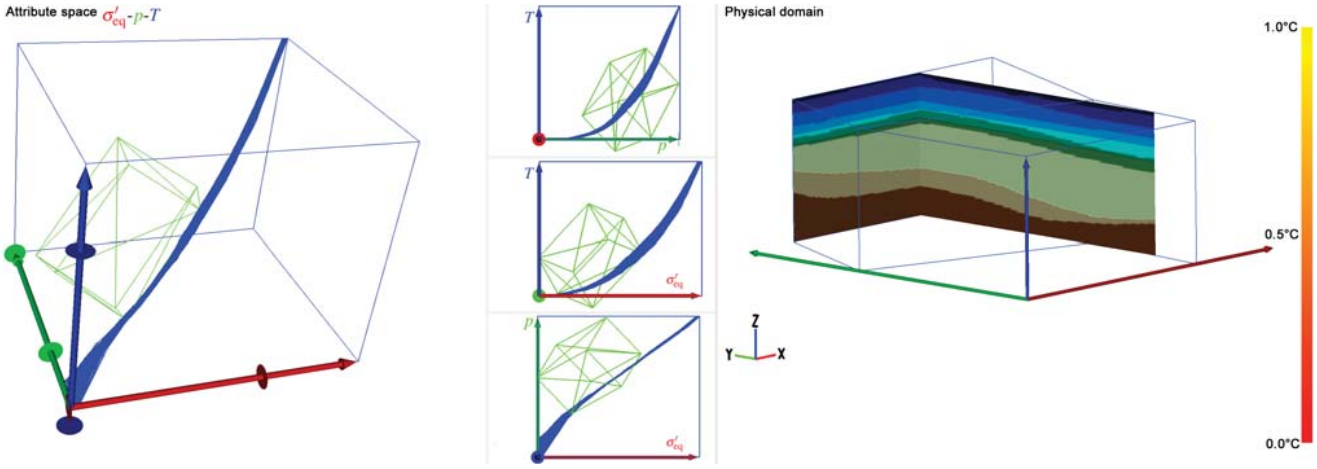

(a) $t = 0$ years

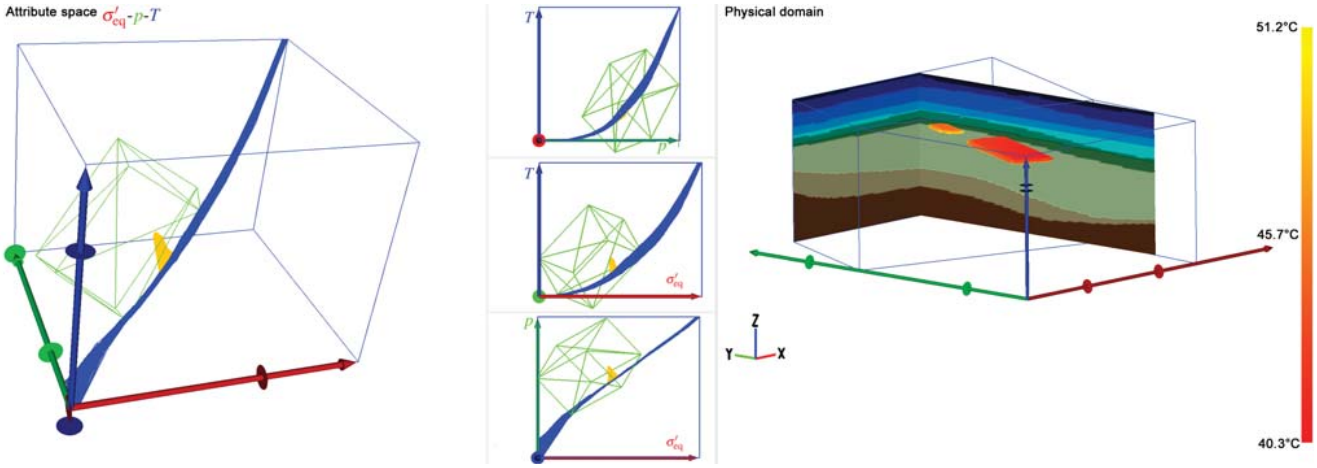

(b) $t = 60$ years

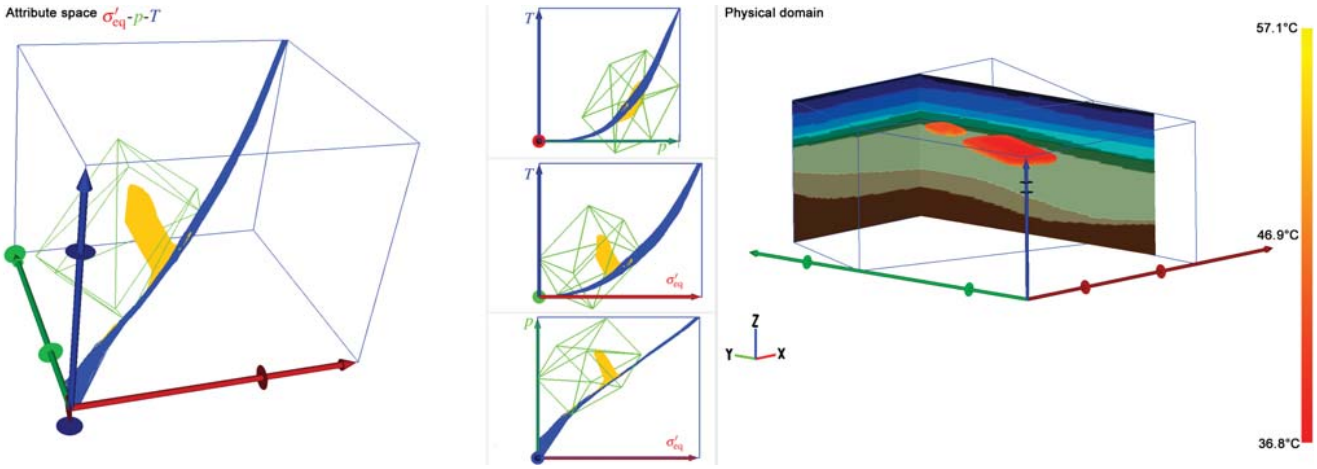

(c) $t = 160$ years

Figure 6. The left hand side of the images shows the σ'_{eq}-p-T state space of the system (σ'_{eq}: $9.13 * 10^5$ Pa - $8.52 * 10^7$ Pa, p: $-4.38 * 10^2$ Pa - $3.73 * 10^7$ Pa, T: 8.0°C - 142.8°C). The right hand side illustrates in Euclidean space the bounding surface of the region marked by the interactor in phase space (green box on the left). The background colors clarify the geological layers for context. For information on the geological layers, see [10]–[12].

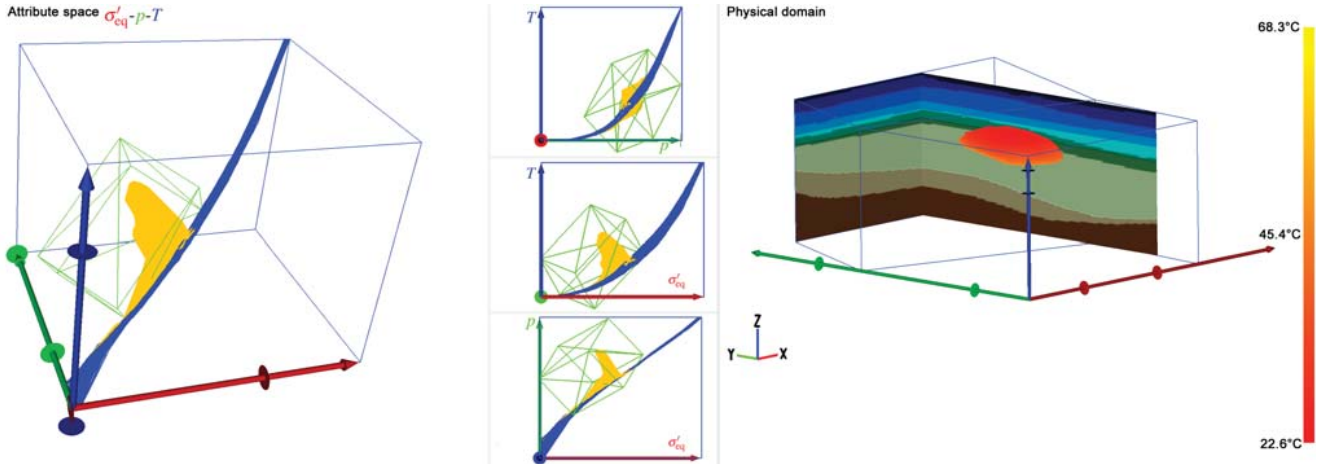

(a) $t = 600$ years

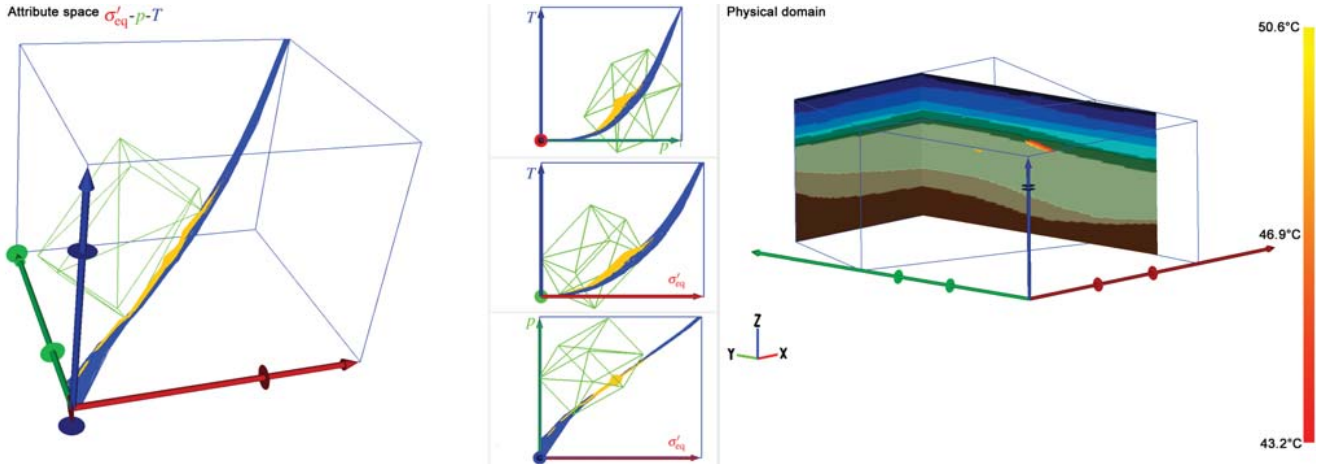

(b) $t = 3500$ years

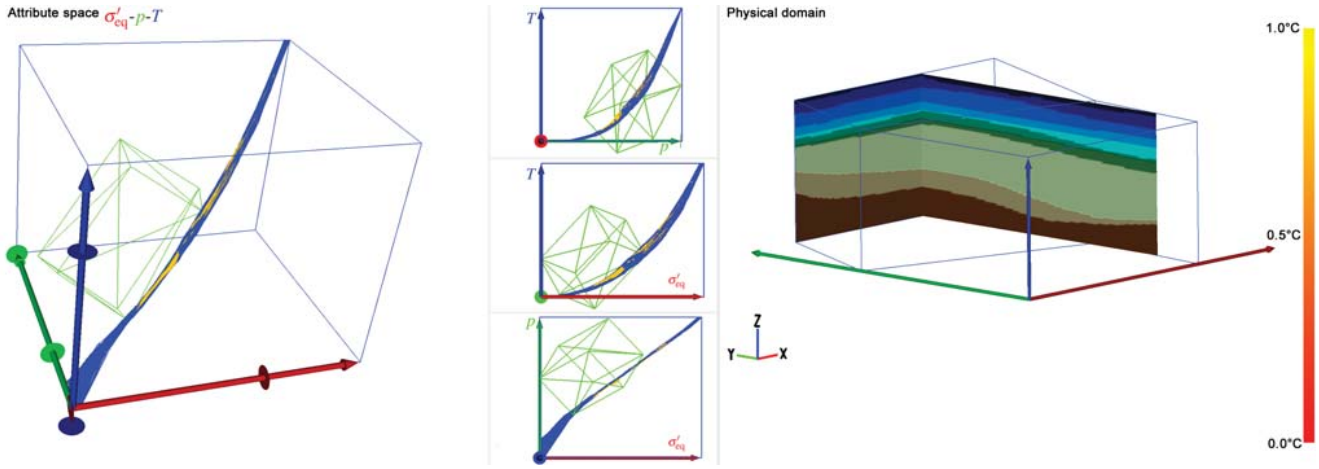

(c) $t = 14000$ years

Figure 7. The left hand side of the images shows the σ'_{eq}-p-T state space of the system (σ'_{eq}: $9.13 * 10^5$ Pa - $8.52 * 10^7$ Pa, p: $-4.38 * 10^2$ Pa - $3.73 * 10^7$ Pa, T: 8.0°C - 142.8°C). The right hand side illustrates in Euclidean space the bounding surface of the region marked by the interactor in phase space (green box on the left). The background colors clarify the geological layers for context. For information on the geological layers, see [10]–[12].